Regulation of Therapeutic Hypothermia on Inflammatory Cytokines, Microglia Polarization, Migration and Functional Recovery after Ischemic Stroke in Mice

Jin Hwan Lee[1,3], **Zheng Z Wei**[1,3], **Wenyuan Cao**[1], **Soonmi Won**[1], **Xiaohuan Gu**[1,3], **Megan Winter**[1], **Thomas A. Dix**[4,5], **Ling Wei**[1,2], and **Shan Ping Yu**[1,3]

[1]Department of Anesthesiology, Emory University School of Medicine, Atlanta, GA, 30322

[2]Department of Neurology, Emory University School of Medicine, Atlanta, GA, 30322

[3]Center for Visual and Neurocognitive, Rehabilitation, Atlanta Veterans Affairs Medical Center, Decatur, GA, 30033

[4]JT Pharmaceuticals, Mt. Pleasant, SC, 29464

[5]Department of Drug Discovery and Biomedical Sciences, Medical University of South Carolina, Charleston, SC 29401

Abstract

Stroke is a leading threat to human life and health in the US and around the globe, while very few effective treatments are available for stroke patients. Preclinical and clinical studies have shown that therapeutic hypothermia (TH) is a potential treatment for stroke. Using novel neurotensin receptor 1 (NTR1) agonists, we have demonstrated pharmacologically induced hypothermia and protective effects against brain damages after ischemic stroke, hemorrhage stroke, and traumatic brain injury (TBI) in rodent models. To further characterize the mechanism of TH-induced brain protection, we examined the effect of TH (at ±33°C for 6 hrs) induced by the NTR1 agonist HPI-201 or physical (ice/cold air) cooling on inflammatory responses after ischemic stroke in mice and oxygen glucose deprivation (OGD) in cortical neuronal cultures. Seven days after focal cortical ischemia, microglia activation in the penumbra reached a peak level, which was significantly attenuated by TH treatments commenced 30 min after stroke. The TH treatment decreased the expression of M1 type reactive factors including tumor necrosis factor-α (TNF-α), interleukin-1β (IL-1β), IL-12, IL-23, and inducible nitric oxide synthase (iNOS) measured by RT-PCR and Western blot analyses. Meanwhile, TH treatments increased the expression of M2 type reactive factors including IL-10, Fizz1, Ym1, and arginase-1. In the ischemic brain and in cortical neuronal/BV2 microglia cultures subjected to OGD, TH attenuated the expression of monocyte

---

#Corresponding author: Shan Ping Yu, M.D., Ph.D., 101 Woodruff Circle, WMR Building Suite 620, Emory University School of Medicine, Atlanta, GA 30322, spyu@emory.edu, Tel. 404-712-8678.

chemoattractant protein-1 (MCP-1) and macrophage inflammatory protein-1α (MIP-1α), two key chemokines in the regulation of microglia activation and infiltration. Consistently, physical cooling during OGD significantly decreased microglia migration 16 hrs after OGD. Finally, TH improved functional recovery at 1, 3, and 7 days after stroke. This study reveals the first evidence for hypothermia mediated regulation on inflammatory factor expression, microglia polarization, migration and indicates that the anti-inflammatory effect is an important mechanism underlying the brain protective effects of a TH therapy.

Keywords

Stroke; Hypothermia; Neurotensin receptor agonist; HPI-201; Inflammation; M1/M2 polarization; microglia migration; functional recovery

Introduction

Stroke is a leading cause of adult death and disability in the United States and around the globe (Go et al., 2014; Murphy et al., 2013). Despite advancements in understanding the pathogenesis and cellular, molecular mechanisms of stroke pathophysiology over the last few decades, thrombolytic therapy with tissue plasminogen activator (tPA) and endovascular recannulation are only FDA-approved clinical treatments for acute stroke. Due to the limited therapeutic window and hemorrhagic risk of tPA, only less than 4% of stroke patients can be benefited with the thrombolytic treatment (Shobha et al., 2011). Therefore, therapies that can benefit more stroke patients are urgently needed.

TH has been incorporated in the American Heart Association guidelines for post-resuscitation care for more than 10 years (Sugerman and Abella, 2009). In clinical practice, mild to moderate hypothermia (3–5°C reduction) is safe and has been used for the treatments of cardiac arrest and neonatal hypoxic-ischemic encephalopathy (Dae et al., 2003; Xiao et al., 2013). Growing evidence from preclinical and clinical studies shows that therapeutic hypothermia (TH), also referred as targeted temperature management (TTM), is a potential effective treatment for stroke (Dietrich and Bramlett, 2010). Compelling evidence from preclinical research in animal models demonstrated marked protective effects against ischemic and hemorrhagic brain damage. TH therapy prevents brain damages through inhibition of multiple pathways such as oxidative stress, inflammatory responses, metabolic disruption, and cell death signals (Choi et al., 2012; Katz et al., 2004; Truettner et al., 2005). TH therapy improves functional outcomes in animal models and human patients of stroke and TBI (Choi et al., 2012; Lee et al., 2014; Polderman et al., 2002). However, hypothermia induction using physical cooling methods such as a cooling pad/blanket are generally slow to reach the target temperature (e.g. 2–8 hr) in humans (Schwab et al., 1998). Although recent methods using intravenous heat-exchange or infusion have provided better and faster control of core temperature (Polderman et al., 2015), the forced cooling commonly triggers body defensive reactions such as shivering and vasoconstriction, making the cooling process and accurate temperature control very challenging. As a result, sedation of general anesthetics and/or muscle relaxants has to be applied, which increased the risk of adverse effects such as lung infection and coagulopathy (Oddo et al., 2016).

Alternatively, pharmacologically induced hypothermia (PIH) targets the brain thermoregulatory center and/or peripheral temperature sensors. This new approach may provide more efficient and safer cooling methods. Among the agents that can be used for PIH, neurotensin receptor 1 (NTR1) agonists are effective compounds that can achieve regulated reductions of body and brain temperatures (Fantegrossi et al., 2005). Our novel neurotensin derivatives such as HPI-201 (formally ABS-201) has the chemical structure of CH3-homolys-Arg-Pro-Tyr-*tert*-Leu-Leu-COOH and can cross the blood brain barrier (BBB). They show high affinity for human NTR1 and induce regulated hypothermia in a dose-dependent manner (Hadden et al., 2005; Orwig et al., 2009). Our group has demonstrated that acute and delayed administrations of HPI-201 and HPI-363 show marked protective effects against brain injury after ischemic and hemorrhagic strokes as well as traumatic brain injury (TBI) in adult and neonatal rodent models (Choi et al., 2012; Lee et al., 2014; Lee et al., 2016b; Wei et al., 2013). NRT1 agonists additionally show antinociceptive and antipsychotic actions (Guillemette et al., 2012; Mechanic et al., 2009). We have identified that the cooling action of the NRT1 compounds, but not their other pharmacological effects, is responsible for observed neuroprotection because when the body temperature is forced to stay at normal level after the drug administration its neuroprotective effect is eliminated (Choi et al., 2012; Gu et al., 2015; Lee et al., 2014; Wei et al., 2013). In addition, we verified that the tested NTR1 compounds do not alter basic physiological parameters including blood pressure, blood glucose, and blood pH, although heart beat increases (Choi et al., 2012; Lee et al., 2014). Therefore, these NTR1 agonists such as HPI-201 are suitable for the induction of TH and HPI-201 was tested in this investigation along with physical (ice/cold air) cooling. Our previous studies demonstrated that the pharmacological TH protects the brain through suppressing apoptosis, autophagy, and BBB damage (Choi et al., 2012; Lee et al., 2014; Wei et al., 2013). However, it is not entirely clear which pathological signaling/s and cellular mechanism/s may be regulated by TH induced by either pharmacological and physical means.

Inflammatory mechanisms are activated after brain ischemia and act as important mediators in the pathogenesis of secondary injury after stroke and TBI (Herz et al., 2014; Vila et al., 2000). Activated glial cells, infiltrated leukocytes, and release of pro-inflammatory cytokines can be detrimental in the ischemic brain and contribute to infarct formation (Sladojevic et al., 2014; Yenari et al., 2010). The inhibition of pro-inflammatory mediator production has been shown to prevent brain injury after stroke (Gelderblom et al., 2012). Microglia is a highly plastic cell with coexisting diverse phenotypes (polarization of M1 and M2) that can be beneficial or detrimental in response to specific microenvironment signals. M1 microglia are considered to be pro-inflammatory and secrete TNF-α, monocyte chemoattractant protein (CCL2/MCP-1) and inducible nitric oxide synthase (iNOS) (Murray and Wynn, 2011). They also express IL-1β, IL-18 and IL-23 through activation of the inflammasome (Ransohoff and Brown, 2012). M2 microglia is thought to be healing cells that are involved with neuroprotection and repair after injury. M2 activation is induced by Th2 cytokines IL-4, IL-13, IL-10, Fizz1, Ym1, or arginase-1, which can enhance the expression of scavenger receptors and pro-angiogenic factors, to have neuroprotective effects. These dual roles of microglia polarization are seen in stroke (Hu et al., 2012; Won et al., 2015). Whether TH,

induced either by physical cooling or pharmacological reagents, may affect microglia activation/polarization has so far not been explored.

In the present study, we specifically tested the effect of TH therapies on inflammatory responses after a hypoxic/ischemic insult in cultured cells as well as in a stroke model of adult mice. Our data provide new evidence that TH can suppress the expression of inflammatory factors, attenuate microglia activation, migration and promote functional recovery after stroke. It is suggested that comprehensive anti-inflammatory effects play a pivotal role in the brain protection achieved by a TH therapy after stroke.

Materials and Methods

Chemicals

The synthesis of proprietary NTR1 agonist HPI-201 was performed using the procedures described previously (Hadden et al., 2005; Orwig et al., 2009). The full chemical structure of HPI-201 was provided in our previous report (Choi et al., 2012).

Animals and focal cerebral ischemic stroke model of mice

Adult male C57BL/6 mice (8–12 weeks, 22–28 g) were used in this study. The mice were housed in standard cages in 12-hr light/12-hr dark cycle in the Emory University animal facility where the room temperature was kept at 22±1°C. Food and water were provided ad libitum. Animals were randomly divided into sham control and experimental groups. In neuroprotection experiments, 6 mice were used in sham control and 12 mice in stroke or stroke plus treatment group. For the measurements of mRNA and protein levels, 3 and 5 animals were included in sham control and stroke/treatment groups, respectively. Immunohistochemical examinations used 7 or 8 mice in each group. In the study on microglia activation, each group contained 3–4 animals. For behavioral tests, 5 mice were tested as sham control and 12 mice were in each stroke/treatment group. In top scan and home cage measurements, 3–5 mice were included in each group.

Focal cerebral ischemic stroke targeting the right somatosensory cortex involving mainly the barrel cortex was induced by occlusion of distal branches of the middle cerebral artery (MCA), as described previously. Animals were anesthetized by 2% isoflurane in 100% Oxygen, followed by a maintenance dose of 1.5% isoflurane. The animal's head was held in a non-invasive holder between the palate and the bridge of the nose without interfering with breathing. A 10-mm incision was made midway between the right eye and ear. The underlying muscle was separated, and a 4-mm diameter circle was incised in the skull with a dental drill with a sterile round 1.5-mm bit to the inner layer of cranium; then the encircled bone was evulsed with a dental tool. The transparent dura was left intact. By videomicroscopy the barrel cortex is localized by intrinsic optical signals (IOS) during whisker stimulation (Wei et al., 1995). Three distal branches of the MCA enclosing the right barrel cortex region were permanently ligated with #10 sterile monofilament sutures through the dura. This was accompanied by 14-min bilateral common carotid artery (CCA) ligation to ensure sufficient local ischemia. The combined occlusions of the MCA and CCA reduces the local blood flow at the targeted cortical area to about 10% of basal flow, leading to

infarct formation in the somatosensory cortex 1 −3 days later (Jiang et al., 2016). The muscle and skin wound was closed with sterile 6-0 sutures. In sham surgical controls, all of these steps were identical and the ligation sutures were placed but not tied shut.

Rectal temperatures in all animals were maintained at 37±0.5°C during surgery using a heating pad controlled by a homeothermic blanket control unit (Harvard Apparatus, Holliston, MA, USA). After surgery, mice were allowed to recover in a humidity-controlled incubator (Thermocare, Incline Village, NV, USA). Animals in sham and stroke groups were injected with saline after surgery, and their body temperatures were maintained at 37±0.5°C in a humidity-controlled incubator for either 6 or 24 hrs. In the hypothermia group, animals were subjected to HPI-201 injections or ice/cold air (4°C) exposure, and no other intervention was applied to influence their body temperatures. Animal protocols were approved by the Emory University Institutional Animal Care and Use Committee (IACUC), in compliance with National Institutes of Health (NIH) guidelines.

Induction of hypothermia using HPI-201

HPI-201 was dissolved in saline and injected intraperitoneally (Choi et al., 2012; Wei et al., 2013). Mice were randomly divided into 4 groups: (1) sham group; (2) stroke group; (3) stroke plus HPI-201 treatment group (6 hr); and (4) stroke plus HPI-201 treatment group (24 hr). For the HPI-201 treatment groups, the first bolus injection (2 mg/kg) was given at 30 min after CCA reperfusion (37 min after the onset of MCA occlusion), followed by additional injections at a half of the initial dose (1 mg/kg). The interval between the injections was 1.5 hr, with adjustments made in order to keep a constant mild hypothermia at 33°C. Rectal temperatures were monitored using a rectal probe (Harvard Apparatus) for 6 hr after CCA reperfusion, and repeated every 15 min for the first hour and every 60 min thereafter. The Physitemp temperature monitoring system (Physitemp Instruments, Inc., Clifton, NJ, USA) allows simultaneous monitoring and data acquisition from seven animals either during or after anesthesia. The implantable thermocouple probe has a tip diameter of 0.16 mm and was placed on the surface of the normal area of the cerebral cortex. The microprobe was contacted to a guide cannula that attached to the caps of two dummy cannulas (model C313 DC, Plastic Products Co., Roanoke, VA, USA). The probe was connected with an extension wire to the data acquisition system controlled by a laptop computer.

TTC staining for the measurement of infarct volume

Three days after the onset of MCA/CCA occlusion, animals in different groups were sacrificed for assessment of brain infarct formation. 2,3,5-triphenyltetrazolium chloride (TTC; Sigma-Aldrich, St. Louis, MO, USA) staining was used to reveal damaged/dead brain tissue as previously described (Choi et al., 2012). Brains were removed, placed in a brain matrix, then sliced into 1-mm coronal sections. Slices were incubated in 2% TTC solution at 37°C for 5 min, then stored in 10% buffered formalin for 24 hr. Digital images of the caudal aspect of each slice were obtained by a flatbed scanner. Infarct, ipsilateral hemisphere, and contralateral hemisphere areas were measured using ImageJ software (NIH, Bethesda, MD, USA). The indirect method (subtraction of residual right hemisphere cortical volume from

cortical volume of the intact left hemisphere) was used to calculate infarct volumes. Infarct measurements were performed under double-blind conditions.

Western blot analysis

Western blot analysis was used to detect the expressions of inflammatory markers. Three animals were included in the sham group, 5 animals in the stroke group, and 5 animals in the stroke plus HPI-201 group. After sacrifice, animals were subjected to transcardial perfusion using phosphate-buffered saline (PBS; pH 7.4). Brain penumbra tissue was lysed in a buffer containing 20 mM $Na_4P_2O_7$, 10 mM Tris-HCl (pH 7.4), 100 mM NaCl, 1 mM EDTA (pH 8.0), 1% Triton, 1 mM EGTA, 2 mM Na_3VO_4, and a protease inhibitor cocktail (Sigma-Aldrich). The supernatant was collected after centrifugation at 15,000 g for 10 min at 4°C. Protein concentration was determined with a bicinchoninic acid assay (Pierce Biotechnology, Rockford, IL, USA). Equivalent amounts of total protein were separated by molecular weight on an SDS-polyacrylamide gradient gel, then transferred to a PVDF membrane. The blot was incubated in 5% bovine serum albumin for 1 hr and then reacted with primary antibodies at 4°C overnight. The primary antibodies used and the dilutions for each were rabbit TNF-α (Cell Signaling, Danvers, MA, USA) at 1:1000, rabbit IL-1β (Cell Signaling) at 1:1000, rabbit IL-6 (Cell Signaling) at 1:1000, mouse anti-IL-10 (Santa Cruz Biotechnology, Inc., Dallas, TX, USA) at 1:500, and mouse anti-actin (Sigma-Aldrich) at 1:5000. After washing with TBST, membranes were incubated with AP-conjugated secondary antibodies (GE Healthcare, Piscataway, NJ, USA) for 1 hr at room temperature. After final washing with TBST, the signals were detected with bromochloroidolylphosphate/nitroblue tetrazolium (BCIP/NBP) solution (Sigma-Aldrich). Signal intensity was measured by ImageJ (NIH) and normalized to the actin signal intensity.

Immunohistochemical staining

Mice were anesthetized with 4% chloral hydrate and perfused with 4% paraformaldehyde. Brains were removed and kept overnight in 4% paraformaldehyde and then transferred to 30% sucrose. Frozen perfusion brain tissues were sliced into 10 μm-thick coronal sections using a cryostat (Leica CM 1950; Leica Microsystems, Buffalo Grove, IL, USA). Sections were dried on the slide warmer for 30 min, fixed with 10% formalin buffer, washed with −20°C precooled ethanol:acetic acid (2:1) solution for 10 min, and finally permeabilized with 0.2% Triton-X 100 solution for 5–10 min. All slides were washed 3 times with PBS (5 min each) after each step. Then, tissue sections were blocked with 1% fish gelatin (Sigma-Aldrich) in PBS for 1 hr at room temperature, and subsequently incubated with the primary antibody ionized calcium binding adaptor molecule 1 (Iba1; 1:600; Biocare Medical, Concord, CA, USA) and NeuN (1:400; Millipore, Billerica, MA, USA) overnight at 4°C. The next day, slides were washed 4 times with PBS for 5 min, then reacted with the secondary antibodies Alexa Fluor®488 goat anti-mouse (1:200; Life Technologies, Grand Island, NY, USA) and Cy3-conjugated donkey anti-rabbit (1:800; Jackson ImmunoResearch Laboratories, West Grove, PA, USA) for 90 min at room temperature. After 4 washings with PBS, nuclei were stained with Hoechst 33342 (1:20,000; Life Technologies) for 5 min as a counterstain, mounted with Vectashield fluorescent mounting medium (Vector Laboratory, Burlingame, CA), and coverslipped for microscopy and image analysis.

Quantification of Iba1 positive cells

Cell counts were performed as described previously, following the principle of design based stereology (Choi et al., 2012). Systematic random sampling was employed to ensure accurate and non-redundant cell counting. Six brain sections per animal were collected at 100 μm distance between sections for non-overlapping multistage random sampling. Six fields were chosen in each section in the penumbra region and viewed at 40x for cell counting. ImageJ (NIH) was used to analyze each picture. The percentage of immunoreactive cells among total Hoechst 33342-positive cells in the penumbra area was counted and summarized in a total of six non-overlapping fields. All analysis was performed in a double-blind fashion. The number of counted cells also was confirmed by two people to verify the accuracy of the result.

Isolation of total RNA and RT-PCR

Total RNA from tissues of stroke mice or neuronal cells was isolated according to manufacturer's instruction (P/N 4387406; A&B Applied Biosystems). RNA integrity was confirmed by detection of 28s and 18s rRNA bands. RNA was confirmed to be free of genomic DNA contamination using PCR in the absence of reverse transcriptase. The RNA samples were reverse transcribed in 20 μl at 37°C for 60 min then incubated at 95°C for 5 min and transferred to 4°C. RT product (1 μl) was subjected to PCR amplification with 10 pmole primer, 10X standard Taq reaction buffer, 10 mM dNTP, and 0.625 unit Taq polymerase in 20 μl PCR reaction buffer (#M0273L, #N0447S, #B9014S; New England Biolabs Inc., Ipswich, MA, USA). PCR primers were used as shown in Table 1 and in our previous study (Chen et al., 2015; Lee et al., 2016a). PCR mixtures were heated to 95°C for 10 min and cycled 30–37 times for each primer; cycles consisted of 95°C for 15 sec, 58°C for 1 min, and 68°C for 30 sec. After additional incubation at 68°C for 10 min, the PCR samples were transferred to 4°C. PCR products were subjected to electrophoresis in 2% agarose gel with ethidium bromide (EtBr). Relative intensity of each PCR band was analyzed using InGenius3 manual gel documentation systems (Syngene, Frederick, MD, USA).

Primary neuronal culture

Cell cultures were isolated from C57BL/6 fetal mice (E16; Charles River) by dissection of the cerebral cortex as previously described with minor modifications (Ogle et al., 2012). Cells were maintained in Neurobasal media with B-27 serum-free culture supplement (Thermo Fisher Scientific, Waltham, MA, USA) and L-glutamine (Thermo Fisher Scientific) until time of experiments. Apoptotic cell death model by B-27 supplement withdrawal was performed on cells after 7 days *in vitro* (DIV); 5 μM cytosine arabinoside (ARA-C; Sigma-Aldrich) was added on day three of culture to halt proliferation of glial cells to provide a nearly pure neuronal population. B-27 contains a mix of necessary anti-oxidant and trophic support components for *in vitro* neuronal cell survival.

BV2 microglial cell lines

BV2 microglia cell line was purchased from American Type Culture Collection (ATCC, Manassas, VA, USA) and cultured in Dulbecco's modified Eagle medium (DMEM)

supplemented with 10% fetal bovine serum. Cell cultures were incubated at 37°C in a 5/95% mixture of CO_2 and atmospheric air; the medium was replaced every 3 days.

Oxygen glucose deprivation (OGD)

To mimic ischemic conditions *in vitro*, an OGD insult was carried out in cortical neuron/glial cultures of DIV 12–13 or in BV2 microglial cell cultures. In OGD groups, media was exchanged for a physiological buffer solution lacking glucose (120 mM NaCl, 25 mM Tris-HCl, 5.4 mM KCl, 1.8 mM $CaCl_2$, pH to 7.4 with NaOH). Cells were then incubated for 3 hr in a calibrated hypoxia chamber perfused with 5% CO_2 and balanced nitrogen for a final ambient oxygen level of 0.2%. Oxygen level was established, maintained, and monitored by the ProOx 360 sensor (Biospherix, NY, USA). After 3 hrs, cells were returned to the normal 5% CO_2 incubator, and the existing OGD media was diluted by half with normal-oxygenated complete neuronal culture media. During OGD, the cells were incubated in the incubator at either 33°C (hypothermia) or 37°C (control). At 24 hrs after OGD, release of lactate dehydrogenase (LDH) into the medium was detected using a cytotoxicity LDH detection kit (Roche, Nutley, NJ, USA). Briefly, 50 μl medium and 50 μl mixture of reagent A and B were co-incubated for 30 min and then absorbance (492 nm) was detected using an Epoch microplate spectrophotometer (BioTek, Winooski, VT, USA). The results were normalized to both the basal LDH release in control cultures (minimum limit) and the LDH release of full kill cultures (maximum limit).

Transwell migration assay in vitro

Cell migration was detected using an *in vitro* Boyden chamber assay and a co-cultivation assay as previously described with minor modification (Won et al., 2015). Microglial cells were suspended in standard medium, and 3×10^4 cells were seeded to the upper well of each transwell insert (Corning Life Sciences, Tewksbury, MA, USA), which bore an uncoated filter with 8-μm diameter holes. At 16 hrs after OGD, these transwells with microglial cells were inserted in the neuronal plate and the lower wells contained only medium. The cell-bearing filters were fixed in 4% paraformaldehyde for 10 min, rinsed with PBS, and the microglia remaining on the upper side of each filter was removed with a Q-tip. The cells migrating to the underside were stained with Hoechst 33342 and counted at 20x magnification with an Olympus BX61 microscope (Olympus, Tokyo, Japan).

Corner test

The corner test was performed 1 day before ischemia and 3 days after ischemia, as described previously (Choi et al., 2012). Two cardboard plates (30 cm x 20 cm x 0.3 cm) were attached at a 30° angle from each other in a home cage. Each subject mouse was placed between the two plates and allowed to freely move to the corner. The number of right and left turns was counted. Twenty trials/tests were performed for each mouse.

Cylinder test

A unilateral injury to the motor cortex results in an asymmetry in the forelimb used for support during rearing, which can be measured using the cylinder test. The mice were placed in a glass cylinder (9.5 cm diameter and 11 cm height) and the number of times each

forelimb or both forelimbs were used to support the body on the wall of the cylinder was counted for 5 min. The animals were evaluated at 1, 3, 7, and 14 days after stroke. Two mirrors were placed behind the cylinder to view all directions. The number of impaired and non-impaired forelimb contacts was calculated as a percentage of total contacts.

Cross beam test

Beam walking across a bridge was performed to assess motor coordination and balance after stroke (Zhu et al., 2008). Mice had pre-training for 3 days before stroke to cross a narrow beam (12 mm diameter and 80 mm in length) to reach their home cage. The mice were placed on one side end of the beam and the time to cross the beam was recorded. Data were expressed as mean time to cross the beam of 3 trials.

Top Scan behavioral tests

Video monitoring system was used to measure motor function after stroke (Clever Sys Inc., Reston, VA, USA). All procedures were carried out in a square open field test chamber (50 cm x 50 cm x 50 cm). Mice were placed in the center of the chamber and allowed to move about freely for 1 hr. Behaviors such as distance, velocity, and turning were recorded using TopScan CleverSys (Clever Sys, Inc.). After finishing the recording, the videos were analyzed by the TopScan Realtime Option Version 3.0 (Clever Sys Inc.). The arena was cleaned with 70% ethanol after each mouse completed a session.

Home Cage behavioral tests

Behavioral changes of mice were monitored and analyzed using the HomeCageScan (Clever Sys Inc.). The system had 4 cameras that monitored 4 cages, with each cage (191mm x 292mm x 127mm) containing one mouse. The behavior patterns were continuously recorded for 12 hr. After finishing the recording, the videos were analyzed by the Home Cage Software 3.0 (Clever Sys Inc.). For this behavioral study, 5–6 animals per group were used.

Statistical analysis

GraphPad Prism 6 (GraphPad Software, San Diego, CA, USA) was used for statistical analysis and graphic presentation. Student's two-tailed t-test was used for comparison of two experimental groups, and One-way ANOVA followed by Bonferroni correction was used for multiple-group comparisons. Two-way ANOVA followed by Bonferroni correction was used for repeated measurements. Significant differences between groups were identified by a P value of <0.05. All data are presented as Mean±SEM.

Results

HPI-201 induced hypothermia in stroke mice

A focal ischemic stroke model was established by permanent occlusion of distal branches of the right MCA plus 14 min CCA bilateral ligations. This ischemic insult selectively damaged the right somatosensory cortex involving the barrel cortex of adult mice (Choi et al., 2012; Ogle et al., 2012). In our previous and current studies, 6-hr mild to moderate hypothermia (2–5°C reduction) induced by NTR1 agonists was applied because similar

degree and duration of physical cooling was neuroprotective against ischemic brain damage in rodents (Choi et al., 2012; Lee et al., 2014; van der Worp et al., 2007; Wei et al., 2013). For comparison, we added a 24-hr hypothermia group in this investigation to determine whether prolonged hypothermia could result in better outcomes after stroke.

An HPI-201 bolus injection (2 mg/kg, i.p.) was given 30 min after CCA reperfusion. Body temperature dropped below 34°C within 15–30 min after injection and was maintained at ~33°C for 6 hrs or 24 hrs by additional injections at a half of the initial dose (1 mg/kg, i.p.) (Fig. 1A). The delayed treatment of 30 min after stroke was selected based on the prediction that the TH treatment using hypothermic drugs such as HPI-201 can be applied on-field soon after the onset of a stroke attack without the need for distinguishing the types of stroke. This is possible because, unlike tPA that can only be used for ischemic stroke, HPI-201 shows protective effects against both ischemic and hemorrhagic strokes (Choi et al., 2012; Lee et al., 2016b; Wei et al., 2013).

Three days after the ischemic insult, brain sections were analyzed for the infarct volume using TTC staining. The infarct volume was significantly reduced in HPI-201 treated TH group compared to that in normothermia stroke controls (Fig. 1B and 1C). Interestingly, 6-hr and 24-hr hypothermia treatments resulted in similar protections; there was no significant difference in the infarction volume between the two groups (Fig. 1B and 1C). In functional assessments 3 days after stroke, stroke control mice exhibited biased turning behavior in the corner test and reduced use of the affected forelimb in the cylinder test (Fig. 1D and 1E). The TH treatment significantly improved functional performance in both tests. Consistent with TTC results, functional performance was similar between the 6-hr and 24-hr TH groups. Thus, in following experiments, 6-hr TH was further tested.

TH therapy altered inflammatory cytokine and chemokine levels

To evaluate the effects of TH on inflammation, we measured the expression levels of some key inflammatory mediators in the peri-infarct region at 3 days after stroke. RT-PCR and Western blotting analyses showed increases in the expression of tumor necrosis factor-α (TNF-α) and interleukin-1β (IL-1β) (Fig. 2A-2C and 2F-2H). The expression ratios of TNF-α and IL-1β in the HPI-201 TH group versus stroke-saline group were significantly decreased to approximately normal levels. On the other hand, the protein and mRNA levels of the anti-inflammation cytokine IL-10 were significantly increased in TH treatment groups (Fig. 2A, 2E, 2F and 2J). There was no significant difference between groups in the expression of IL-6 protein (Fig. 2A and 2D), although the IL-6 mRNA level showed a marked decrease in the stroke brain, which was prevented by the TH treatment (Fig. 2F and 2I).

Monocyte chemoattractant protein-1 (MCP-1) and macrophage inflammatory protein-1α (MIP-1α) are key chemokines that regulate migration and infiltration of microglia and monocytes. Three days after stroke, RT-PCR analysis revealed that the ischemic insult significantly raised the MCP-1 and MIP-1α expression in the peri-infarct region, while HPI-201 remained their mRNA levels as seen in sham controls (Fig. 2K-2M).

TH therapy attenuated microglia activation

Microglia activation plays important roles in the pathogenesis of stroke (Yenari et al., 2010). Immunostaining of the ionized calcium binding adaptor molecule 1 (Iba1) was measured in peri-infarct region at 2, 3, 7, 14, and 21 days after stroke (Fig. 3A-3C). Microglia cell density increased at 2 days after stroke and reached its peak at day 7 (Fig. 3C). In the TH group received HPI-201 treatment, the density of Iba1-positive microglia cells was significantly reduced at 3 and 14 days compared to stroke controls at the same time points (Fig. 3D).

TH therapy regulated M1/M2 polarization

To examine the effect of TH on M1/M2 microglia/macrophage polarity, we used well-defined M1/M2 markers in addition to general inflammatory cytokine/chemokine markers. In RT-PCR assays, the expression of M1 markers IL-23, IL-12, and iNOS in the ischemic cortex increased 3 days after stroke (Fig. 4A and 4B). These increases were significantly attenuated by HPI-201-induced TH. Furthermore, the TH treatment increased the M2 markers Fizz1, Ym1, and arginase-1 after stroke (Fig. 4A and 4B). Similar regulation of the inflammatory factors by physical cooling was observed, although in a less intense manner (Fig. 4C).

TH regulation of cytokine/chemokine expression and microglia migration after OGD in neuronal and BV2 microglial cultures

To verify the direct effect of hypothermia on cell viability and inflammatory factors, *in vitro* ischemic model OGD was tested in cortical neuronal cell cultures. In the hypothermia group, culture dishes were kept at 33°C by ice and cold air exposure during 3-hr OGD. Cell death assays using the LDH measurement at 24 hrs after OGD showed that hypothermia significantly prevented OGD-induced neuronal death (Fig. 5B). Similar to the observation in stroke animals, OGD provoked MCP-1 and MIP-1α expression in neurons whereas cooling suppressed their levels in these cells (Fig. 5A).

Microglia migration is a key player of the brain responses to injury and inflammation (Block and Hong, 2005). To verify whether hypothermia could attenuate microglial migration, OGD was tested in co-cultivation of neuronal and BV2 microglial cells using the transwell migration assay. Migration of BV-2 microglial cells across transwell membranes increased 16 hrs after OGD, whereas cooling to 33°C during OGD caused a significant reduction in migration at this delayed time point (Fig. 5C and 5D).

TH therapy improved motor function after stroke

To examine functional outcomes after stroke, the cylinder and cross beam tests were performed. Stroke animals that received the HPI-201-induced TH showed significantly better performance in the cylinder test at 1 and 3 days after stroke (Fig. 6A). HPI-201 treatment significantly increased the rate of impaired limb use compared with saline treated stroke mice. Walking across a bridge was used to assess motor coordination and balance (Zhu et al., 2008). Stroke mice spent prolonged time to cross the bridge, while those received the TH treatment finished the test much faster than stroke control mice (Fig. 6B). The significant differences between groups in functional performance showed a time-

dependent disappearance due to spontaneous recovery of the motor function at 7 or 10 days after stroke (Fig. 6B).

TH therapy improved general behaviors and home cage activities after stroke

Functional and behavioral activities of stroke animals in their home cage environment was monitored using a top scan camera and a home cage monitoring system (Steele et al., 2007). Walking distance and velocity and turning behavior were captured for 1 hr at 3 days after stroke. Stroke mice exhibited reduced walking distance, slower velocity, and less turns compared with sham control mice. Stroke animals that received HPI-201 treatment reverted to normal activity levels in these behaviors (Fig. 6C).

The home cage monitoring was repeated at 7 days after stroke. At this delayed time point, abnormal and depression-like behaviors persisted or developed in stroke animals, including shorter walking distance, prolonged inactive time spent in rest/stationary and reduced activities in rearing, grooming, hanging, and jumping (Fig. 7). They also showed less turns compared with sham animals. Stroke mice received the TH treatment, on the other hand, appeared normal in these behavioral activities (Fig. 7).

Discussion

Accumulating and compelling evidence has endorsed that TH is a promising therapeutic strategy after cardiac arrest and likely for brain injuries including stroke and TBI (Dietrich and Bramlett, 2010; Piironen et al., 2014; Su et al., 2016; Xiao et al., 2013). The cellular mechanism of the TH protection can be multifaceted, such as reduced death of multiple cells involving necrosis, apoptosis and autophagy, and prevention of brain edema and BBB damage. In the present study, we specifically evaluated the anti-inflammatory effects of TH therapies using pharmacological means and physical cooling. The main findings are that TH shows a profound regulatory effect on inflammatory response, including the inhibition of the M1 polarization of microglia accompanied with reduced expression of TNF-α, IL-1β, IL-23, IL-12, and iNOS. Meanwhile, TH enhances M2 transition, shown as increased production of IL-10, Fizz1, Ym1, and arginase-1. Detailed experiments in cultured cells exposed to OGD with and without cooling reveal that TH attenuates migration/recruitment of microglia via suppression of inflammatory factors and reduced microglia migration. Finally, a TH treatment promotes functional recovery after stroke. These data all support that TH therapy can regulate stroke related inflammatory activities, and the TH anti-inflammation action is beneficial for brain protection and functional improvements after stroke.

Post-stroke events such as excitotoxicity, oxidative stress, and production of reactive oxygen species lead to inflammatory responses (Yoshino et al., 1997). During ischemia, inflammation is characterized by the production of various inflammatory cytokines such as TNF-α, IL-1β, IL-6, and IL-10, the accumulation of neutrophils, and the activation of microglia in the injured brain (Huang et al., 2006). In our study, increased Iba1 immunoreactivity was observed at 3 and 7 days after stroke, which was attenuated by an early TH intervention for 6 hrs. Stroke increased the expressions of pro-inflammatory cytokines such as TNF-α and IL-1β, as shown in our RT-PCR and Western blot analyses. These pro-inflammatory cytokines are produced by activated microglia/macrophages and

many other cell types, mediating various cell signaling such as apoptosis and oxidative stress (Doyle et al., 2008; Morganti-Kossmann et al., 2001). The expression of TNF-α and IL-1β was reduced by TH therapy, which is consistent with previous reports using physical cooling (Frink et al., 2012). The expression of IL-10 has been shown to be cellular protective after brain injurious insults such as stroke and TBI but is controversial during or after hypothermia (Kline et al., 2002; Stewart et al., 2010). Consistent with our previous finding in TBI model (Lee et al., 2014), we observed elevated expression of IL-10 in the TH group after stroke. Our findings suggest that TH can help to reduce the microglial activation yet increase anti-inflammatory factor/s after stroke.

Microglia/macrophages are plastic cells with diverse phenotypes that can be involved in the generation of distinct effector cells and functions (Hu et al., 2012; Murray and Wynn, 2011). The chronic activation of microglia may cause neuronal damage through the release of potentially cytotoxic molecules such as pro-inflammatory cytokines, ROS, proteinases and complement proteins (Gordon et al., 2016). Therefore, suppression of microglia-mediated inflammation has emerged as an important strategy in stroke therapy. Anti-inflammatory interventions have been shown to repress the microglial activation and to exert neuroprotective effects after brain injuries (Lucas et al., 2006; Truettner et al., 2005; Webster et al., 2009). Various cytokines and microbial products produced by various stimuli lead to the development of M1 and/or M2 subtypes, which can express different levels of cell surface markers and secrete mediators such as scavenger receptors, chemokines, and cytokines (Gao et al., 2016). M1 polarization is closely associated with pro-inflammatory responses and tissue damage, whereas M2 polarization is more closely linked to an anti-inflammatory role (Hu et al., 2012; Murray and Wynn, 2011). Stroke reinforced M1 microglia reactions and decreased M2 microglia markers, whereas TH counteracts these effects. After stroke induction in rodents, an increased M1 polarization contributes to the inflammatory cascade and propagated cell death beyond the initial ischemic region (Pan et al., 2015; Won et al., 2015). Mice that lack appropriate signals for M2 induction have worse outcomes after cerebral ischemia. For example, IL-4 or IL-10 deficient animals show worse functional recovery after stroke induction (Perez-de Puig et al., 2013; Xiong et al., 2011). In the present study, we reveal the alterations of M1/M2 microglial polarization in the stroke brain and the regulatory effects of TH on these alterations after stroke. Taken together, our current data suggest that TH can suppress inflammatory responses via regulation or alteration of M1/M2 microglial activation after stroke, thus favoring protective and repairing processes.

One possible explanation for the TH effect of shifting microglia from M1 to M2 reaction is its regulation on the cytokine-dependent environment changes (Davis et al., 2013). Previous studies showed that continued production of cytokines such as interferon gamma (IFNγ) and TNF-α induce and maintain M1 polarization states . Ischemia-mediated neuronal damage induces the synthesis and release of chemokines, as primarily secreted small proteins, such as MCP-1, MIP-1α, and interferon-inducible protein (IP-10) in stroke animal models and stroke patients, which recruit microglia, monocytes, and neutrophils (Flugel et al., 2001; Rappert et al., 2004). MCP-1 knockout mice exhibited reduced infarct volume and inhibited acute injury after ischemia (Hughes et al., 2002). In addition, MIP-1α can lead to recruitments of monocyte/macrophage and microglial cells both *in vitro* and *in vivo* (Skuljec

et al., 2011; Wang et al., 2008). MIP-1α exacerbated brain infarction but viral MIP-2 (vMIP-2), a chemokine receptor antagonist, protected neurons against ischemic damages (Takami et al., 2001; Wang et al., 2008). In the present study, upregulations of MCP-1 and MIP-1α expressions in neurons were observed both *in vivo* after stroke and *in vitro* after OGD. Based on the current literature and our findings, we suggest that TH can regulate M1 and M2 microglia types via suppressing neuronal death and altering pro- and anti-inflammatory cytokines.

In previous studies, HPI-201-induced TH treatment improved sensorimotor function in the sticky dot test (Choi et al., 2012; Wei et al., 2013). In the present investigation, results from cylinder and crossbeam behavioral tests showed improved locomotion recovery. Furthermore, the home cage monitoring system provided information on these behaviors with little human intervention. A number of behavioral measurements show that stroke mice had prolonged inactive time compared with sham animals, while stroke mice that received TH treatment appeared normal in these behaviors. Taken together, the TH treatment promotes better functional recovery, and its effect on inflammatory reaction is likely a major contributor to the therapeutic benefit.

Although there is strong evidence from animal studies that TH improves outcomes after cerebral ischemia, clinical trials using physical/forced cooling treatments have shown mixed results. A recent paper by Nielsen et al. reported that, in unconscious cardiac arrest patients, TTM of physical cooling to 33°C did not confer additional benefit as compared with a TTM intervention at 36°C; although the study clearly indicated the importance of controlling the post-stroke fever (hyperpyrexia) (Nielsen et al., 2013). There were questions regarding the selection of patients and data analysis in this investigation (Subramaniam et al., 2015). For example, the mortality of patient groups was noticeably lower than that in other trials, suggesting a possible bias in medical/environment conditions. A TH treatment usually increases the incidence of pneumonia (Geurts et al., 2014), while the Nielsen investigation did not see this complication or other infections in the 33°C group. The delayed achievement to the targeted temperature could be another factor that influences the outcomes of the patients. Thus, the Nielsen study appears inconclusive and more clinical research is needed. Another recent trial reported no significant benefits for mortality rate or neurological functions in stroke patients received TH of physical cooling (Wan et al., 2014). It is commonly agreed that early treatment after acute stroke is critical for brain protection and functional recovery. In most cases of Wan study, TH was initiated 6 to 12 hrs after the onset of stroke, which was likely too late and missed the therapeutic window for the acute treatment of ischemic stroke. Using hypothermic NTR1 agonists, TH intervention can be commenced as an on-site or on-field treatment before or soon after the patient arrival at hospital. This significant advantage of early treatment and faster cooling effect of NTR1 drugs provides greater potential for successful clinical translation of TH therapy for acute stroke patients.

The optimal duration of TH therapy for stroke treatment has been incompletely defined and data from animal and human studies are noticeably different (van der Worp et al., 2010; van der Worp et al., 2007; Wan et al., 2014). Investigations on rodent stroke models showed that 2–3 hr mild hypothermia commenced at ischemic onset was sufficient for neuroprotection

(Maier et al., 2001; Markarian et al., 1996). In some reports, neuroprotection was observed with as brief as 0.5 hr mild hypothermia (Krieger and Yenari, 2004). In a few preclinical studies of focal cerebral ischemia where the length of hypothermia was compared, 1–3 hr hypothermia appeared effective, whereas 0.5–1 hr short cooling was not (Maier et al., 1998; Zhang et al., 1993). Longer durations may be necessary when the initiation of cooling is delayed (Colbourne et al., 2000; Colbourne et al., 1999). In clinical investigations on acute stroke patients, TH is usually applied for extensive duration of 1 to 2 days or even up to 14 day (MacLellan et al., 2009; Marion and Bullock, 2009). This is mostly due to the consideration that 1) post-stroke fever may last for days after stroke (Karaszewski et al., 2013; Phipps et al., 2011), and 2) most stroke patients arrive at hospital several hours after attack so prolonged hypothermia is expected to be necessary. It is possible that the optimal duration of a TH treatment depends on multiple factors, such as the severity of ischemia, the types of stroke (ischemic and hemorrhagic), the occurrence of reperfusion and the delay from the onset of a stroke attack. We consistently demonstrate in rodent stroke models that 6-hr TH induced by hypothermic drugs or physical means initiated 30–60 min after ischemia shows significant neuroprotective and functional benefits (Choi et al., 2012; Jiang et al., 2016). Although we did not see additional benefits with 24-hr hypothermia in the current investigation, it remains to be tested whether prolonged hypothermia may be necessary with more delayed treatments and whether it can show improved outcomes that were not measured in our experiments. It should be mentioned that the therapeutic window and the TH duration illustrated in animal models should be re-established in stroke patients under clinical settings.

Although a long cooling time seems a logic approach, its therapeutic effect may be offset by increased risks of complications accompanied with prolonged cooling procedures. Specifically, clinical hypothermia is usually performed under sedation with sedatives, analgesics and/or paralytic agents in order to combat the reactive vasoconstriction and shivering. This would likely introduce additional burdens and risks, and render neurological monitoring difficult. This complexity could have negative impacts on the outcomes of stroke patients. For example, either cooling or the antishivering regimen, or both, increased the risk of pneumonia (Lyden et al., 2014). Since the centrally acting NTR1 agonists do not cause shivering while inducing efficient and manageable cooling and rewarming (Choi et al., 2012; Lee et al., 2014), application of TH therapy to awaken stoke patients using these hypothermic drugs soon after a stroke attack may allow for shorter duration of TH (e.g. 6–10 hrs) that is sufficient for protective effects, better outcomes and less side-effects after stroke.

Acknowledgments

Abbreviations

ANOVA   analysis of variance

BBB	blood-brain barrier
CCA	common carotid artery
Iba1	ionized calcium binding adaptor molecule 1
IFNγ	interferon gamma
IL-1β	interleukin-1β
IL-6	interleukin-6
IL-10	interleukin-10
IL-12	interleukin-12
IL-23	interleukin-23
iNOS	inducible nitric oxide synthase
IOS	intrinsic optical signals
IP-10	interferon-inducible protein
MCP-1	monocyte chemoattractant protein-1
MIP-1α	macrophage inflammatory protein-1α
NT	neurotensin
NTR1	neurotensin receptor 1
PIH	pharmacologically induced hypothermia
TH	therapeutic hypothermia
TNF-α	tumor necrosis factor-α
TTC	2,3,5-triphenyltetrazolium chloride
TTM	targeted temperature management

References

Block ML, Hong JS. Microglia and inflammation-mediated neurodegeneration: multiple triggers with a common mechanism. Prog Neurobiol. 2005; 76:77–98. [PubMed: 16081203]

Chen D, et al. Intranasal Delivery of Apelin-13 Is Neuroprotective and Promotes Angiogenesis After Ischemic Stroke in Mice. ASN Neuro. 2015:7.

Choi KE, et al. A novel stroke therapy of pharmacologically induced hypothermia after focal cerebral ischemia in mice. FASEB J. 2012; 26:2799–2810. [PubMed: 22459147]

Colbourne F, et al. Prolonged but delayed postischemic hypothermia: a long-term outcome study in the rat middle cerebral artery occlusion model. J Cereb Blood Flow Metab. 2000; 20:1702–1708. [PubMed: 11129786]

Colbourne F, et al. Indefatigable CA1 sector neuroprotection with mild hypothermia induced 6 hours after severe forebrain ischemia in rats. J Cereb Blood Flow Metab. 1999; 19:742–749. [PubMed: 10413028]

Dae MW, et al. Safety and efficacy of endovascular cooling and rewarming for induction and reversal of hypothermia in human-sized pigs. Stroke. 2003; 34:734–738. [PubMed: 12624300]

Davis MJ, et al. Macrophage M1/M2 polarization dynamically adapts to changes in cytokine microenvironments in Cryptococcus neoformans infection. MBio. 2013; 4:e00264–e00313. [PubMed: 23781069]

Dietrich WD, Bramlett HM. The evidence for hypothermia as a neuroprotectant in traumatic brain injury. Neurotherapeutics. 2010; 7:43–50. [PubMed: 20129496]

Doyle KP, et al. Mechanisms of ischemic brain damage. Neuropharmacology. 2008; 55:310–318. [PubMed: 18308346]

Fantegrossi WE, et al. Antinociceptive, hypothermic, hypotensive, and reinforcing effects of a novel neurotensin receptor agonist, NT69L, in rhesus monkeys. Pharmacol Biochem Behav. 2005; 80:341–349. [PubMed: 15680187]

Flugel A, et al. Neuronal MCP-1 expression in response to remote nerve injury. J Cereb Blood Flow Metab. 2001; 21:69–76. [PubMed: 11149670]

Frink M, et al. Facts and fiction: the impact of hypothermia on molecular mechanisms following major challenge. Mediators Inflamm. 2012; 2012:762840. [PubMed: 22481864]

Gao J, et al. Human Neural Stem Cell Transplantation-Mediated Alteration of Microglial/Macrophage Phenotypes after Traumatic Brain Injury. Cell Transplant. 2016

Gelderblom M, et al. The flavonoid fisetin attenuates postischemic immune cell infiltration, activation and infarct size after transient cerebral middle artery occlusion in mice. J Cereb Blood Flow Metab. 2012; 32:835–843. [PubMed: 22234339]

Geurts M, et al. Therapeutic hypothermia and the risk of infection: a systematic review and meta-analysis. Crit Care Med. 2014; 42:231–242. [PubMed: 23989182]

Go AS, et al. Heart disease and stroke statistics--2014 update: a report from the american heart association. Circulation. 2014; 129:e28–e292. [PubMed: 24352519]

Gordon R, et al. Protein kinase Cdelta upregulation in microglia drives neuroinflammatory responses and dopaminergic neurodegeneration in experimental models of Parkinson's disease. Neurobiol Dis. 2016; 93:96–114. [PubMed: 27151770]

Gu X, et al. Pharmacologically induced hypothermia attenuates traumatic brain injury in neonatal rats. Exp Neurol. 2015; 267:135–142. [PubMed: 25725354]

Guillemette A, et al. Intrathecal administration of NTS1 agonists reverses nociceptive behaviors in a rat model of neuropathic pain. Eur J Pain. 2012; 16:473–484. [PubMed: 22396077]

Hadden MK, et al. Design, synthesis, and evaluation of the antipsychotic potential of orally bioavailable neurotensin (8–13) analogues containing non-natural arginine and lysine residues. Neuropharmacology. 2005; 49:1149–1159. [PubMed: 16095636]

Herz J, et al. Exacerbation of ischemic brain injury in hypercholesterolemic mice is associated with pronounced changes in peripheral and cerebral immune responses. Neurobiol Dis. 2014; 62:456–468. [PubMed: 24184800]

Hu X, et al. Microglia/macrophage polarization dynamics reveal novel mechanism of injury expansion after focal cerebral ischemia. Stroke. 2012; 43:3063–3070. [PubMed: 22933588]

Huang J, et al. Inflammation in stroke and focal cerebral ischemia. Surg Neurol. 2006; 66:232–245. [PubMed: 16935624]

Hughes PM, et al. Monocyte chemoattractant protein-1 deficiency is protective in a murine stroke model. J Cereb Blood Flow Metab. 2002; 22:308–317. [PubMed: 11891436]

Jiang MQ, et al. Long-term Survival and Regeneration of Neuronal and Vasculature Cells inside the Core Region after Ischemic Stroke in Adult Mice. Brain Pathol. 2016

Karaszewski B, et al. Relationships between brain and body temperature, clinical and imaging outcomes after ischemic stroke. J Cereb Blood Flow Metab. 2013; 33:1083–1089. [PubMed: 23571281]

Katz LM, et al. Regulated hypothermia reduces brain oxidative stress after hypoxic-ischemia. Brain Res. 2004; 1017:85–91. [PubMed: 15261103]

Kline AE, et al. Acute systemic administration of interleukin-10 suppresses the beneficial effects of moderate hypothermia following traumatic brain injury in rats. Brain Res. 2002; 937:22–31. [PubMed: 12020858]

Krieger DW, Yenari MA. Therapeutic hypothermia for acute ischemic stroke: what do laboratory studies teach us? Stroke. 2004; 35:1482–1489. [PubMed: 15073396]

Lee JH, et al. Neonatal inflammatory pain and systemic inflammatory responses as possible environmental factors in the development of autism spectrum disorder of juvenile rats. J Neuroinflammation. 2016a; 13:109. [PubMed: 27184741]

Lee JH, et al. Therapeutic effects of pharmacologically induced hypothermia against traumatic brain injury in mice. J Neurotrauma. 2014; 31:1417–1430. [PubMed: 24731132]

Lee JH, et al. Improved therapeutic benefits by combining physical cooling with pharmacological hypothermia after severe stroke in rats. Stroke. 2016b; 47:1907–1913. [PubMed: 27301934]

Lucas SM, et al. The role of inflammation in CNS injury and disease. Br J Pharmacol. 2006; 147(Suppl 1):S232–S240. [PubMed: 16402109]

Lyden PD, et al. Endovascular therapeutic hypothermia for acute ischemic stroke: ICTuS 2/3 protocol. Int J Stroke. 2014; 9:117–125. [PubMed: 24206528]

MacLellan CL, et al. Use of prolonged hypothermia to treat ischemic and hemorrhagic stroke. J Neurotrauma. 2009; 26:313–323. [PubMed: 19216634]

Maier CM, et al. Optimal depth and duration of mild hypothermia in a focal model of transient cerebral ischemia: effects on neurologic outcome, infarct size, apoptosis, and inflammation. Stroke. 1998; 29:2171–2180. [PubMed: 9756600]

Maier CM, et al. Delayed induction and long-term effects of mild hypothermia in a focal model of transient cerebral ischemia: neurological outcome and infarct size. J Neurosurg. 2001; 94:90–96. [PubMed: 11147904]

Marion D, Bullock MR. Current and future role of therapeutic hypothermia. J Neurotrauma. 2009; 26:455–467. [PubMed: 19292697]

Markarian GZ, et al. Mild hypothermia: therapeutic window after experimental cerebral ischemia. Neurosurgery. 1996; 38:542–550. discussion 551. [PubMed: 8837807]

Mechanic JA, et al. Involvement of the neurotensin receptor 1 in the behavioral effects of two neurotensin agonists, NT-2 and NT69L: lack of hypothermic, antinociceptive and antipsychotic actions in receptor knockout mice. Eur Neuropsychopharmacol. 2009; 19:466–475. [PubMed: 19223157]

Morganti-Kossmann MC, et al. Role of cerebral inflammation after traumatic brain injury: a revisited concept. Shock. 2001; 16:165–177. [PubMed: 11531017]

Murphy SL, et al. Deaths: final data for 2010. Natl Vital Stat Rep. 2013; 61:1–126.

Murray PJ, Wynn TA. Protective and pathogenic functions of macrophage subsets. Nat Rev Immunol. 2011; 11:723–737. [PubMed: 21997792]

Nielsen N, et al. Targeted temperature management at 33 degrees C versus 36 degrees C after cardiac arrest. N Engl J Med. 2013; 369:2197–2206. [PubMed: 24237006]

Oddo M, et al. Optimizing sedation in patients with acute brain injury. Crit Care. 2016; 20:128. [PubMed: 27145814]

Ogle ME, et al. Inhibition of prolyl hydroxylases by dimethyloxaloylglycine after stroke reduces ischemic brain injury and requires hypoxia inducible factor-1alpha. Neurobiol Dis. 2012; 45:733–742. [PubMed: 22061780]

Orwig KS, et al. Comparison of N-terminal modifications on neurotensin(8–13) analogues correlates peptide stability but not binding affinity with in vivo efficacy. J Med Chem. 2009; 52:1803–1813. [PubMed: 19290594]

Pan J, et al. Malibatol A regulates microglia M1/M2 polarization in experimental stroke in a PPARgamma-dependent manner. J Neuroinflammation. 2015; 12:51. [PubMed: 25889216]

Perez-de Puig I, et al. IL-10 deficiency exacerbates the brain inflammatory response to permanent ischemia without preventing resolution of the lesion. J Cereb Blood Flow Metab. 2013; 33:1955–1966. [PubMed: 24022622]

Phipps MS, et al. Epidemiology and outcomes of fever burden among patients with acute ischemic stroke. Stroke. 2011; 42:3357–3362. [PubMed: 21980196]

Piironen K, et al. Mild hypothermia after intravenous thrombolysis in patients with acute stroke: a randomized controlled trial. Stroke. 2014; 45:486–491. [PubMed: 24436240]

Polderman KH, et al. Ultrarapid Induction of Hypothermia Using Continuous Automated Peritoneal Lavage With Ice-Cold Fluids: Final Results of the Cooling for Cardiac Arrest or Acute ST-Elevation Myocardial Infarction Trial. Crit Care Med. 2015; 43:2191–2201. [PubMed: 26196354]

Polderman KH, et al. Effects of therapeutic hypothermia on intracranial pressure and outcome in patients with severe head injury. Intensive Care Med. 2002; 28:1563–1573. [PubMed: 12415442]

Ransohoff RM, Brown MA. Innate immunity in the central nervous system. J Clin Invest. 2012; 122:1164–1171. [PubMed: 22466658]

Rappert A, et al. CXCR3-dependent microglial recruitment is essential for dendrite loss after brain lesion. J Neurosci. 2004; 24:8500–8509. [PubMed: 15456824]

Schwab S, et al. Moderate hypothermia and brain temperature in patients with severe middle cerebral artery infarction. Acta Neurochir Suppl. 1998; 71:131–134. [PubMed: 9779165]

Shobha N, et al. Thrombolysis at 3–4.5 hours after acute ischemic stroke onset--evidence from the Canadian Alteplase for Stroke Effectiveness Study (CASES) registry. Cerebrovasc Dis. 2011; 31:223–228. [PubMed: 21178345]

Skuljec J, et al. CCL5 induces a pro-inflammatory profile in microglia in vitro. Cell Immunol. 2011; 270:164–171. [PubMed: 21620385]

Sladojevic N, et al. Inhibition of junctional adhesion molecule-A/LFA interaction attenuates leukocyte trafficking and inflammation in brain ischemia/reperfusion injury. Neurobiol Dis. 2014; 67:57–70. [PubMed: 24657919]

Steele AD, et al. The power of automated high-resolution behavior analysis revealed by its application to mouse models of Huntington's and prion diseases. Proc Natl Acad Sci U S A. 2007; 104:1983–1988. [PubMed: 17261803]

Stewart CR, et al. Hypothermia increases interleukin-6 and interleukin-10 in juvenile endotoxemic mice. Pediatr Crit Care Med. 2010; 11:109–116. [PubMed: 19602992]

Su Y, et al. Improved Neurological Outcome With Mild Hypothermia in Surviving Patients With Massive Cerebral Hemispheric Infarction. Stroke. 2016; 47:457–463. [PubMed: 26696645]

Subramaniam A, et al. Is cooling still cool? Ther Hypothermia Temp Manag. 2015; 5:13–16. [PubMed: 25423577]

Sugerman NT, Abella BS. Hospital-based use of therapeutic hypothermia after cardiac arrest in adults. J Neurotrauma. 2009; 26:371–376. [PubMed: 19231920]

Takami S, et al. Chemokine receptor antagonist peptide, viral MIP-II, protects the brain against focal cerebral ischemia in mice. J Cereb Blood Flow Metab. 2001; 21:1430–1435. [PubMed: 11740204]

Truettner JS, et al. The effect of therapeutic hypothermia on the expression of inflammatory response genes following moderate traumatic brain injury in the rat. Brain Res Mol Brain Res. 2005; 138:124–134. [PubMed: 15922484]

van der Worp HB, et al. Therapeutic hypothermia for acute ischemic stroke: ready to start large randomized trials? J Cereb Blood Flow Metab. 2010; 30:1079–1093. [PubMed: 20354545]

van der Worp HB, et al. Hypothermia in animal models of acute ischaemic stroke: a systematic review and meta-analysis. Brain. 2007; 130:3063–3074. [PubMed: 17478443]

Vila N, et al. Proinflammatory cytokines and early neurological worsening in ischemic stroke. Stroke. 2000; 31:2325–2329. [PubMed: 11022058]

Wan YH, et al. Therapeutic hypothermia (different depths, durations, and rewarming speeds) for acute ischemic stroke: a meta-analysis. J Stroke Cerebrovasc Dis. 2014; 23:2736–2747. [PubMed: 25238926]

Wang HK, et al. Free radical production in CA1 neurons induces MIP-1alpha expression, microglia recruitment, and delayed neuronal death after transient forebrain ischemia. J Neurosci. 2008; 28:1721–1727. [PubMed: 18272692]

Webster CM, et al. Inflammation and NFkappaB activation is decreased by hypothermia following global cerebral ischemia. Neurobiol Dis. 2009; 33:301–312. [PubMed: 19063968]

Wei L, et al. Ministrokes in rat barrel cortex. Stroke. 1995; 26:1459–1462. [PubMed: 7631353]

Wei S, et al. Acute and delayed protective effects of pharmacologically induced hypothermia in an intracerebral hemorrhage stroke model of mice. Neuroscience. 2013; 252:489–500. [PubMed: 23912033]

Won S, et al. Recombinant tissue plasminogen activator promotes, and progesterone attenuates, microglia/macrophage M1 polarization and recruitment of microglia after MCAO stroke in rats. Brain Behav Immun. 2015; 49:267–279. [PubMed: 26093305]

Xiao G, et al. Safety profile and outcome of mild therapeutic hypothermia in patients following cardiac arrest: systematic review and meta-analysis. Emerg Med J. 2013; 30:91–100. [PubMed: 22660549]

Xiong X, et al. Increased brain injury and worsened neurological outcome in interleukin-4 knockout mice after transient focal cerebral ischemia. Stroke. 2011; 42:2026–2032. [PubMed: 21597016]

Yenari MA, et al. Microglial activation in stroke: therapeutic targets. Neurotherapeutics. 2010; 7:378–391. [PubMed: 20880502]

Yoshino H, et al. Postischemic accumulation of lipid peroxidation products in the rat brain: immunohistochemical detection of 4-hydroxy-2-nonenal modified proteins. Brain Res. 1997; 767:81–86. [PubMed: 9365018]

Zhang ZG, et al. Duration dependent post-ischemic hypothermia alleviates cortical damage after transient middle cerebral artery occlusion in the rat. J Neurol Sci. 1993; 117:240–244. [PubMed: 8410062]

Zhu W, et al. Insulin growth factor-1 gene transfer enhances neurovascular remodeling and improves long-term stroke outcome in mice. Stroke. 2008; 39:1254–1261. [PubMed: 18309153]

Highlights

- Pharmacological and physical TH treatments are protective against ischemic stroke.

- TH reduces the expression of inflammatory factors.

- TH regulates microglial M1/M2 polarization and migration.

- TH improves functional recovery after stroke.

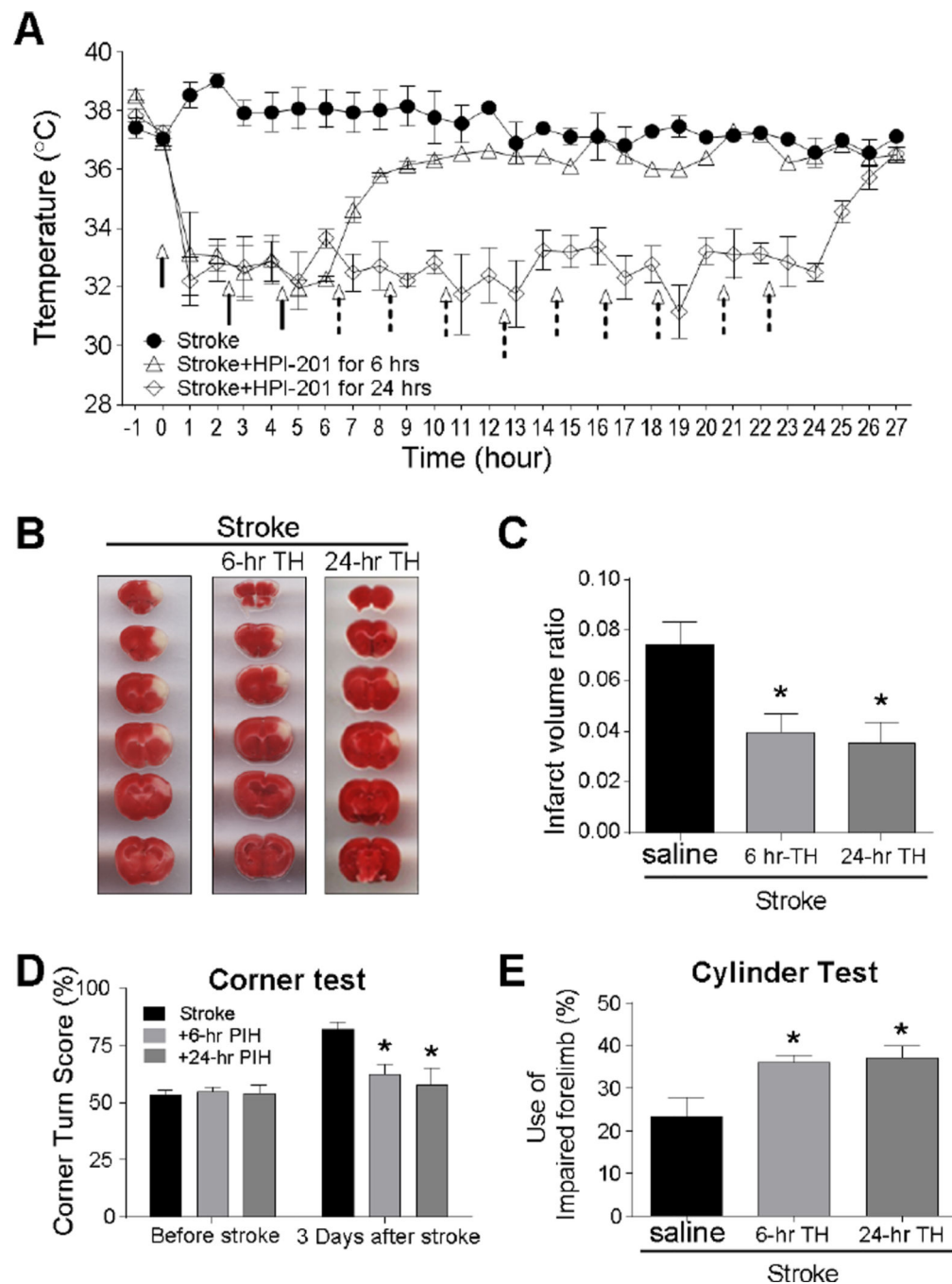- The anti-inflammatory effect of TH is a brain protective mechanism after stroke.

Figure 1. Neuroprotection induced by 6-hr and 24-hr pharmacological TH in stroke mice
The hypothermic effect of the NTR1 agonist HPI-201 in stroke mice. **A**. HPI-201 treatment
(2 mg/kg, i.p.) or saline control was started 30 min after the onset of ischemia. The body
temperature was monitored using a rectal probe, showing induced cooling from 37°C to
33°C in around 30 min. The cooling effect was maintained for 6 or 24 hr by additional
injections (arrows with solid or dotted lines for 6 and 24 hr treatments, respectively). After
the last injection, the body temperature gradually returned to normal level. * $P<0.05$ vs.
stroke group; n=6–12 per group. **B**. TTC staining of brain sections at 3 days after stroke.

Representative images show brain sections from saline, HPI-201-treated for 6 hr (6-hr TH), and HPI-201-treated for 24 hr (24-hr TH) after stroke. **C**. The bar graph summarizes the infarct volume ratio in stroke mice of different groups. Both HPI-201-treated groups with 6 or 24 hr cooling showed significant reduction in the infarct volume. * $P<0.05$ vs. stroke controls; n=6–12 per group. There was no significant difference between 6 and 24 hr groups. **D** and **E**. Corner and cylinder tests were performed 3 days after stroke to compare functional benefits induced by 6 and 24 hr hypothermia. The corner test revealed a bias in the turning direction of stroke animals. Normal animal makes equal left and right turns (50% score in the test). After stroke, animal more likely turned to using the damaged brain side (right side in this study), and the HPI-201 treatment largely prevented this abnormal behavior. In the cylinder test, the increased score illustrated increased use of the affected limb. There were no significant differences between the TH treatment of 6 and 24 hrs. * $P<0.05$ vs. stroke group; n=6–8 per group.
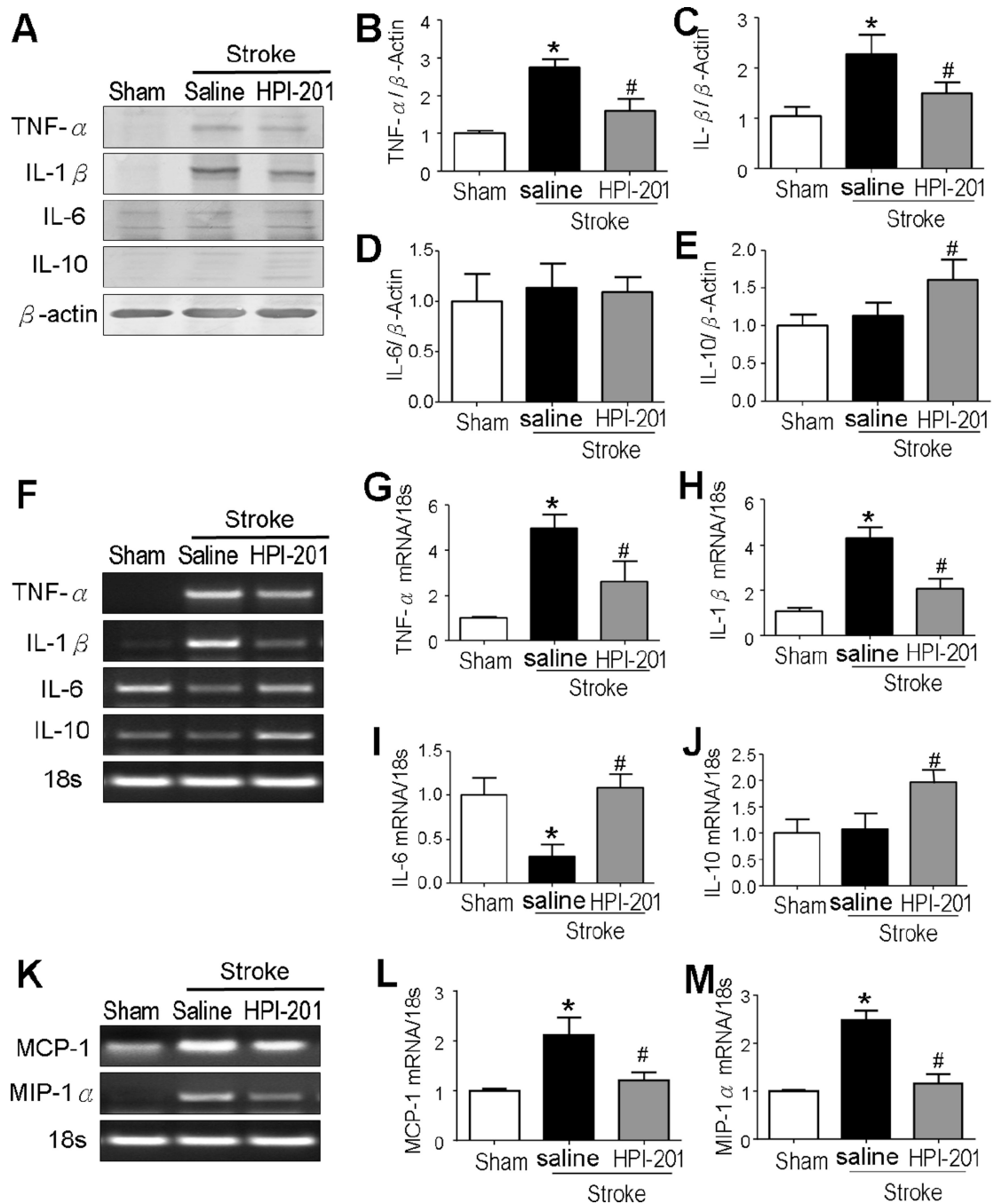
Figure 2. TH altered cytokine expressions in the ischemic brain

Protein expressions (A to E) and mRNA levels (F to M) of cytokines were measured using Western blot and RT-PCR analyses in the penumbra tissue at 3 days after stroke. **A** to **C**. Stroke induction significantly enhanced expression of the pro-inflammatory proteins TNF-α (A and B) and IL-1β (A and C), which was attenuated by the HPI-201 treatment. **D**. No change was observed in the anti-inflammation cytokine IL-6 between groups after stroke. **E**. Stroke did not induce the expression of IL-10, while HPI-201 showed a significant increase in IL-10 expression. * $P<0.05$ versus sham controls; #$P<0.05$ versus stroke controla; n=3 in

sham group, n=5 in stroke and stroke plus HPI-201 groups, respectively. **F** to **J**. RT-PCR analysis of inflammatory cytokines showed that stroke induction increased pro-inflammatory cytokines including TNF-α and IL-1β mRNA, while HPI-201 largely prevented these increases (G and H). Reduced IL-6 mRNA was seen in the stroke brains, while HPI-201 maintained the IL-6 mRNA expression at normal levels (I). There was no change in the anti-inflammation cytokine IL-10 after stroke, while HPI-201 treatment enhanced IL-10 mRNA expression (J). * P<0.05 versus sham group; # P<0.05 versus stroke group; n=3–5 per group. **K** to **M**. RT-PCR analysis of chemokines showed upregulations of MCP-1 and MIP-1α after stroke, which were blocked by HPI-201 treatment. * P<0.05 versus sham group; # P<0.05 versus stroke group; n=5 per group.
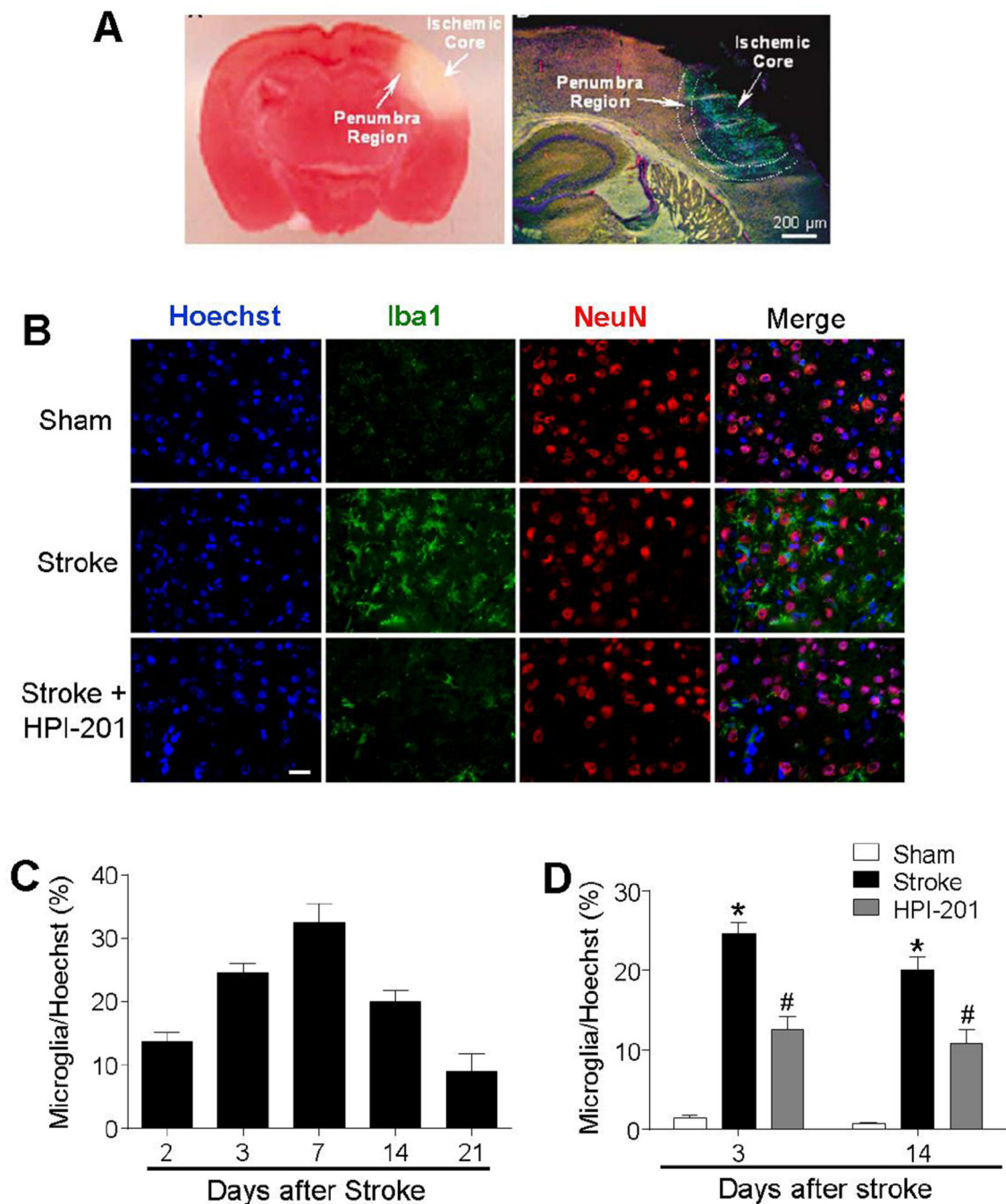
Figure 3. TH reduced microglial activation in the ischemic brain

Cell type identification and regulation in the peri-infarct (penumbra) region of the post-stroke brain. **A**. Left: TTC staining 24 hrs after ischemia showing the ischemic core and the peri-infarct region. The pink area between the normal cortex and ischemic core represents the bordering penumbra area. Right: A brain section at lower magnification shows the massive cell death (TUNEL-positive cells of green color) in the ischemic core and scattered cell death in penumbra 3 days after ischemia. Red: Glut-1 staining of vascular endothelial cells, Blue: NeuN staining of neurons. **B**. Representative images showing immunostaining of

Iba1 (green), NeuN (red), and Hoechst 33342 (blue) at 3 days after stroke. **C**. The time course of microglia recruitment to the penumbra region 2 to 21 days after stroke. **D**. Effects of HPI-201 and vehicle treatment on microglia recruitment. HPI-201 attenuated the number of Iba1-positive microglial cells at 3 and 7 days after stroke. * P<0.05 versus sham group; #P<0.05 versus stroke group; n=7–8 per group. Scale bars = 20 μm.
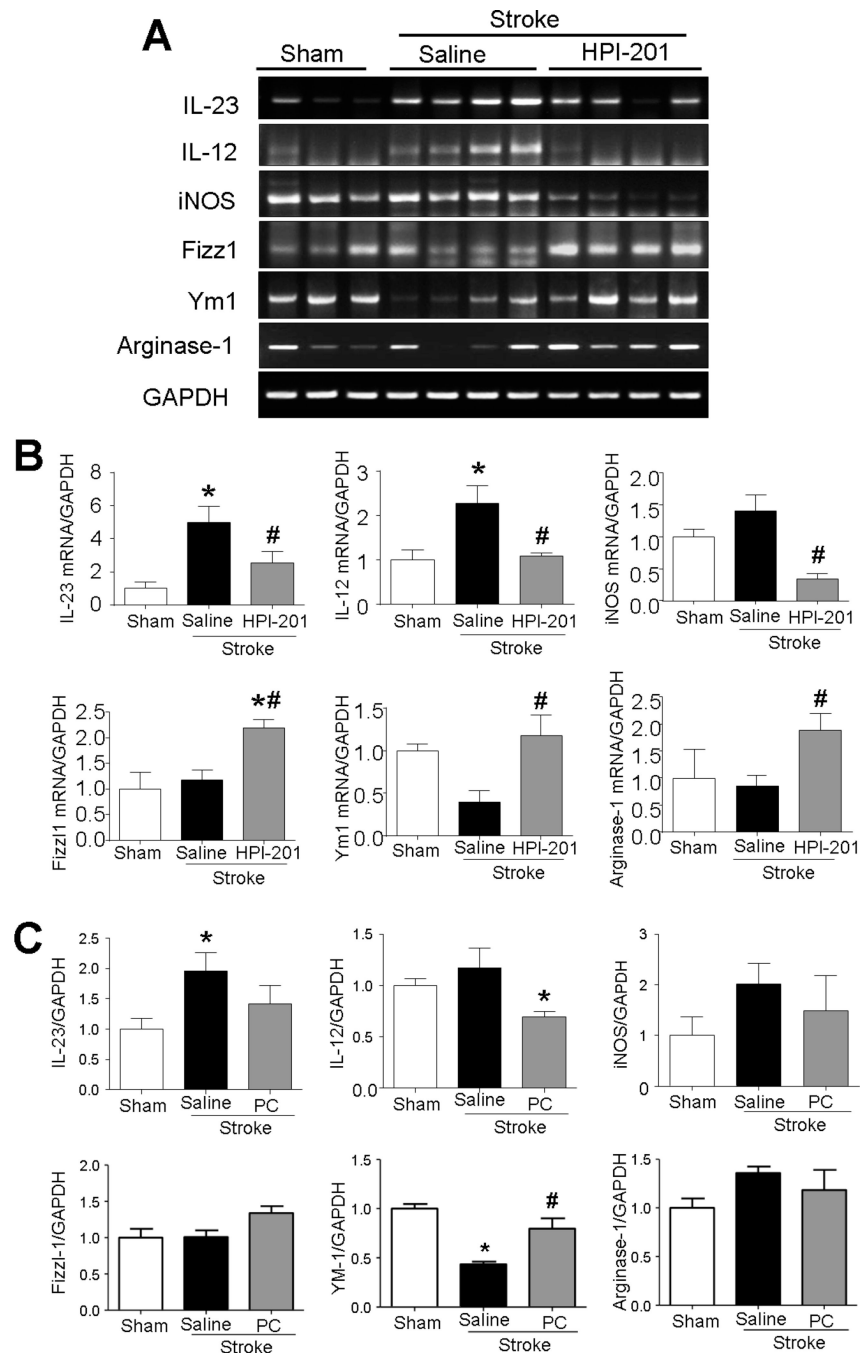
Figure 4. Effects of TH on M1/M2 polarization of microglia after stroke
The mRNA expressions of M1/M2 polarization markers of microglia were measured using RT-PCR analysis in the penumbra region at 3 days after stroke induction. **A**. RT-PCR analysis of various M1 (IL-23, IL-12, and iNOS)/M2 (Fizz1, Ym1, and arginase-1) polarization markers of microglia. **B**. Summarized RT-PCR assays in HPI-201-induced TH experiments. Stroke increased M1 polarization cytokines and decreased M2 polarization cytokines, while HPI-201 significantly recovered M1/M2 polarization. * $P<0.05$ versus sham group; # $P<0.05$ versus stroke group; n=3–4 per group. **C**. Summarized RT-PCR

assays in physical cooling (PC) induced TH experiments. While stroke increased the level of IL-23, IL-12, and iNOS, cooling significantly reduced IL-12 expression and showed trend of reducing IL-23 and iNOS in microglia cells. PC also increased the M2 marker YM-1.
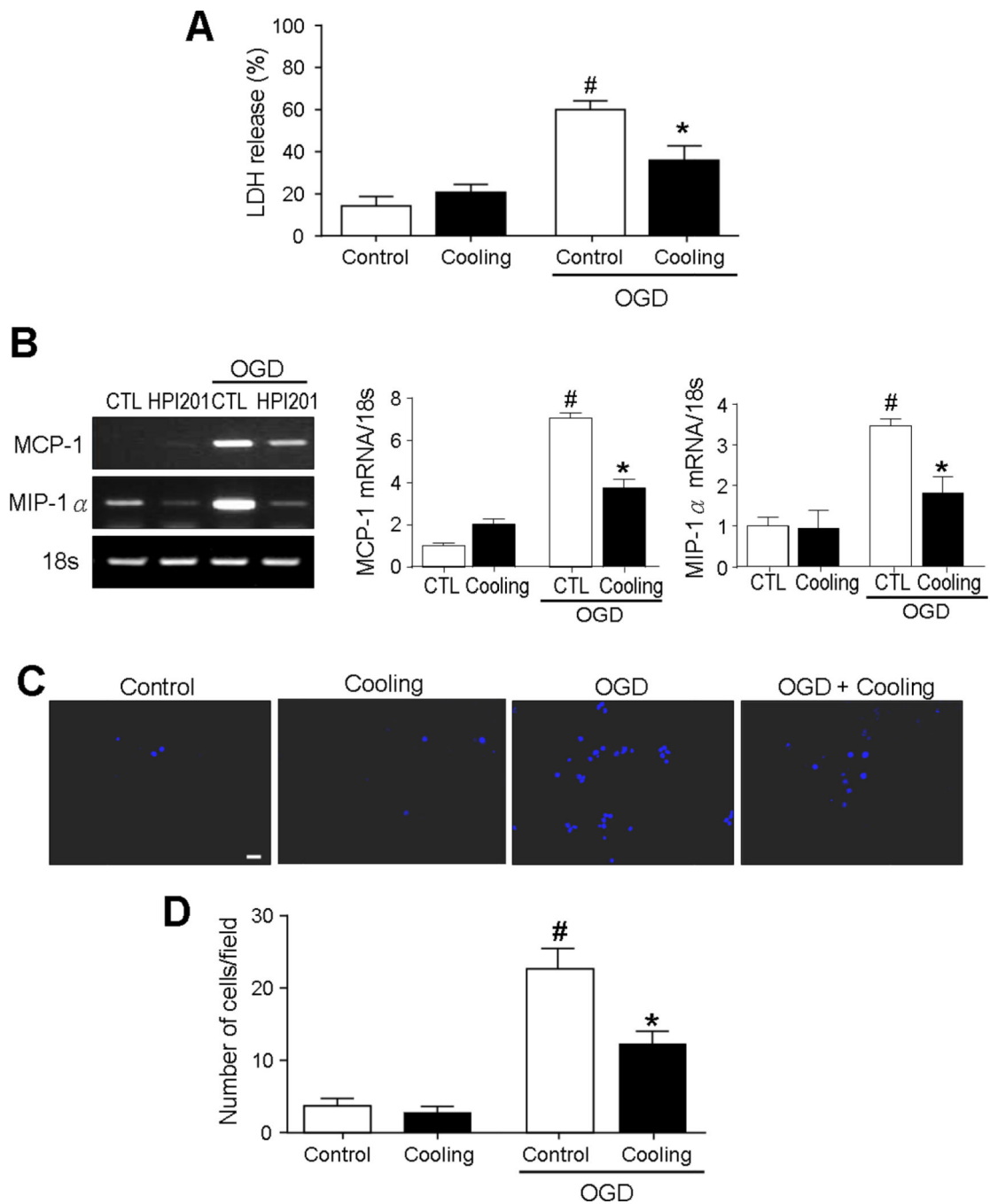
Figure 5. Effects of TH on chemokines activity and microglia migration after OGD in neuronal and BV2 microglial cell cultures

The cooling effects on inflammatory responses were examined in cultured neuronal and BV2 microglial cells subjected to OGD. Physical cooling was achieved using a hypothermic incubator (33°C, 5% CO_2) during OGD. **A**. OGD led to significant neuronal death, but the increase was attenuated by hypothermia. # $P<0.05$ versus no OGD groups; * $P<0.05$ versus OGD control group; n=3 per group. **B**. MCP-1 and MIP-1α mRNA levels in control (CTL) and hypothermia (cooling) groups, as determined by RT-PCR analysis. Reducing the

medium temperature to 33°C during OGD decreased MCP-1 and MIP-1α increases in neuronal cells. # $P<0.05$ versus no OGD groups; * $P<0.05$ versus OGD control group; n=3 per group. **C**. Representative photographs of the transmigrated Hoechst 33342-labeled microglia under each condition in a Transwell chamber. Scale bars = 20 μm. **D**. Quantified graphs of the number of the transmigrated microglia in co-cultivation of neuronal and/or BV2 microglial cells. # $P<0.05$ versus no OGD groups; * $P<0.05$ versus OGD control group; n=3 per group.
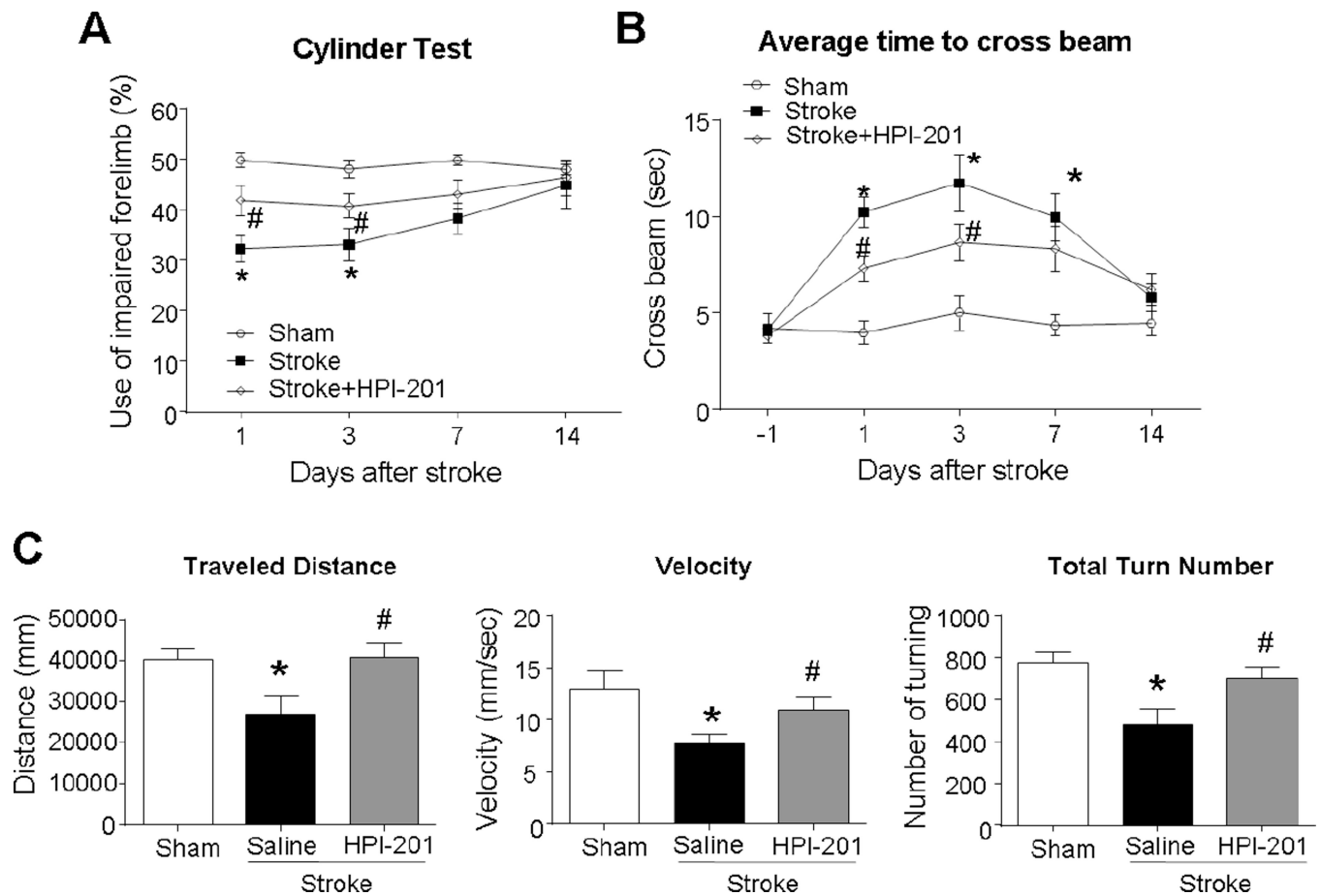
Figure 6. TH improved locomotor functional recovery after stroke

Cylinder and crossbeam tests were used to evaluate motor functional recovery after stroke induction. **A**. Cylinder test showed that forelimb activities of stroke mice were impaired during the first few days after stroke. Mice that received HPI-201 performed significantly better than stroke controls. The difference disappeared 7 days after stroke due to spontaneous recovery in this moderate stroke model. * $P<0.05$ versus sham group; # $P<0.05$ versus stroke group; n=5–12 per group. **B**. Crossbeam tests showed that stroke damage led to prolonged time to cross the beam compared with sham group at 1, 3, 7 days after stroke. However, stroke mice that received HPI-201 demonstrated significantly reduced time to cross the beam. * $P<0.05$ versus sham group; # $P<0.05$ versus stroke group; n=5–12 per group. **C**. Locomotor activity was examined in an open field container (50 × 50 × 50 cm). In the TopScan monitoring analysis performed 3 days post-stroke, mice showed reduced distance, slower velocity, and less turning, while mice that received HPI-201 were unaffected. * $P<0.05$ versus sham group; # $P<0.05$ versus stroke group; n=5–6 per group.
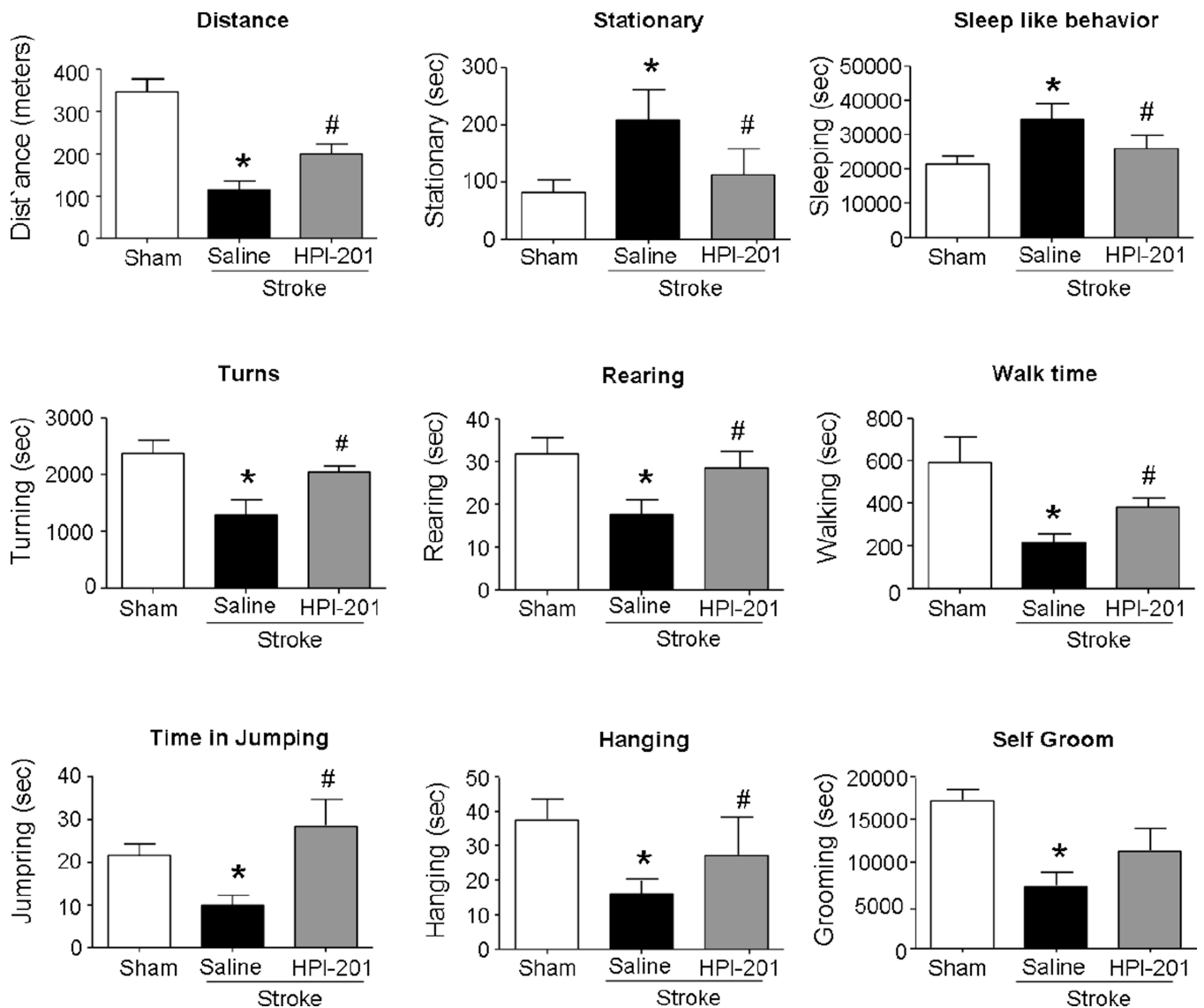
Figure 7. TH improved home cage behaviors of stroke mice
Home cage monitoring system was performed to measure the more accurate and entire functional recovery after stroke induction in mice. Twelve hour home cage monitoring system enabled the analysis of both active behaviors such as rearing, grooming, hanging, and jumping, and the inactive behaviors such as sleeping-like and stationary activities. At 7 days after stroke induction, injured mice showed shorter traveled distance and prolonged inactive time, while mice with HPI-201 treatment appeared normal in these behaviors. * $P<0.05$ versus sham group; # $P<0.05$ versus stroke group; n=5–6 per group.

Table 1

RT-PCR primers used in the study

Genes		Primers 5′-3′
TNF-α	Forward	GATCTCAAAGACAACCAACTAGTG
	Reverse	CTCCAGCTGGAAGACTCCTCCCAG
IL-β	Forward	TCGGCCAAGACAGGTCGCTCA
	Reverse	TGGTTGCCCATCAGAGGCAAGG
IL-6	Forward	GAGGATACCCCCAACAGACC
	Reverse	AAGTGCATCATCGTTGTTCATACA
IL-10	Forward	ATGAAGGTCTCCACCACTG
	Reverse	GCATTCAGTTCCAGGTCAC
MCP-1	Forward	ATGCAGGTCCCTGTCATG C
	Reverse	GCTTGAGGTGGTTGTGGAG
MIP-1α	Forward	CACCCACTTCCCAGTCGGCCA
	Reverse	TGCTTCTCTGCCGGCATCAC
IL-23	Forward	GACTGTTGCCTCTCGTACA
	Reverse	CGACTGTTGCCTCTCGTACA
IL-12	Forward	AAATGAAGCTCTGCATCCTGC
	Reverse	TCACCCTGTTGATGGTCACG
iNOS	Forward	GCAGAATGTGAGCATCATGG
	Reverse	ACAACCTTGGTCTTGAAGGC
Fizz1	Forward	TCCCAGTGAATACTGATGAGA
	Reverse	CCACTCTGGATCTCCCAAGA
Ym1	Forward	GGGCATACCTTTATCCTGAG
	Reverse	CCACTGAAGTCATCCATGTC
Arginase-1	Forward	CGCCTTTCTCAAAAGGACAGC
	Reverse	CAGCTCTTCATTGGCTTTCAC
18s	Forward	GACTCAACACGGGAAACCTC
	Reverse	ATGCCAGAGTCTCGTTCGTT
GAPDH	Forward	ACCACAGTCCATGCCATCAC
	Reverse	CACCACCCTGTTGCTGTAGCC